Journal of Mechanical Engineering Research Vol. 4(2), pp. 36-46, February 2012
Available online at http://www.academicjournals.org/JMER
DOI: 10.5897/JMER11.065
ISSN 2141-2383 ©2012 Academic Journals

Full Length Research Paper

Transient and dynamic performance of solar driven multiple effect distillation

Ashraf S. Hassan* and Hassan E. S. Fath

Masdar Institute of Science and Technology, Abu-Dhabi, United Arab Emirate.

Accepted 19 December, 2011

Transient and dynamic performance of solar driven multiple-effect distillation (MED) system without thermal energy storage (storing of water rather than energy) are studied and presented. A typical 25,900 m^3/day operational multiple effect distillation with thermal vapor compression (MED-TVC) is used for the transient and dynamic simulation. Two scenarios are studied for the transient performance to; i) pump the feed water flow and ii) spray feed water onto the horizontal tubes bundle in each effect. The first scenario uses a constant flow rate of feed water along most of operating hours. The second scenario assumes a sinusoidal trend for the feed water flow rate during the operating hours (simulating direct PV electrical generation with no electric energy storage). The dynamic performance is due to a disturbance of a rectangular pulse forcing function on the seawater flow for duration of 50 s, which increased 25% for 5 s. The response of that disturbance on the behavior of the MED process parameters, such as the distributions of the temperatures, mass flow rates, and physical properties is presented. The physical model of each effect is divided into seven compartments including brine pool, vapor space, tubes bundles and feed water pre-heater. Transient and dynamic equations for each compartment and other system components are formulated mathematically. Mass, salt and energy balance equations are solved dynamically taking into consideration the inter-related effect of each compartment onto the other. The transient resultant flow rates of each stream (vapor production, TVC, brine disposal, etc) are presented in details and compared to conventional steady operation. When using the feed water scenario of sinusoidal feed to operate the solar MED unit, the results indicates that the salt precipitation can increase above the designed value. The results show also that the dynamic behavior of feeding water coming into the effects is flows the same trend the disturbance that took place in the main source of seawater supply. The flow rates of feed water are affected by the applied disturbance and increases gradually from normal operation to a peak value then decreases again to the normal operation state value. The system undergoes this disturbance shows to be still stable in operation as the change in its behavior is just bounded around the disturbance time, and regain, in a very short time, to the initial (normal operation) value of starting point.

Key words: Solar energy, desalination, dynamic behavior, MED-TVC.

INTRODUCTION

Multiple effect distillation with thermal vapour compression (MED-TVC) is a commonly used technology and is particularly attractive due to its high performance ratio with lower number of effects, good flexibility to load variation, and is a stable system. Solar driven desalination plants have a large potential application in GCC and MENA countries due to the availability of suitable solar intensity and the serious fresh water shortage. Solar desalination has also international interest as it reduces the CO_2 emission and the global warming and adds to

*Corresponding author. E-mail: asadik@masdar.ac.ae.

the required reduction of CO_2 footprint. Solar thermal energy can be directly used to drive desalination systems as in solar stills (by humidification (H) and dehumidification (HD) process) to obtain distilled water. However, majority of larger scale application of solar desalination use solar energy indirectly. In addition to the widely used solar PV-RO systems, Solar thermal integrated with MSF and MED can suits the harsh water need in the GCC countries. In these systems, solar energy is harvested by using non-concentrating or concentrating solar collectors. The collected solar thermal energy can then be used to drive thermal desalination methods such as MSF, MED, vapor compression (VC) or membrane distillation (MD) (Hassan et al., 2008). A review of solar collectors is provided in Al-Hallaj et al. (2006). In Kalogirou (2004), a general discussion of efforts made for using renewable energy sources such as solar, wind, geothermal and wave for desalination is presented. Tauha et al. (2011) presented a comprehensive study on the indirect solar driven desalination systems.

Solar – MED has been selected in the present study as MED proved to be reliable and matured commercial technology that suits integration with low temperature solar system. In addition, MED consumes lower specific electrical energy consumption than MSF (and require lower cost of solar PV) and has the potential increase in GOR with higher TBT (easily available in medium temperature solar thermal systems). Mabrouk et al. (2008) studied the techno-economics of typical operation MED unit with mechanical vapor compression.

El-Nashar (2008) presented Umm El-Nar Solar-MED plant in Abu Dhabi, UAE. The plant has been operating successfully for 18 years to demonstrate supplying fresh water using solar thermal energy. The economic feasibility of the plant was established by comparing the cost of water from a solar MED plant with a conventional MED plant capacity ranging from 100 to 1000 m^3/d. It was found that the cost of water from solar MED plant is only competitive with that from a conventional MED plant if the cost fuel continues to rise to $100/barrel, which exceeds this value now. This study was only concerned with steady state normal operation solar MED system.

Process dynamic, on the other hand, is concerned with analyzing the time-dependent behavior of an energy process in response to various types of inputs. The main objective of dynamic simulation analysis is to investigate and characterize system behavior when a process is subjected to various types of input changes. Dynamic process mathematical models are usually addressed in the form of differential equations: linear and non-linear, ordinary and partial.

Hassan and Hanafi (2007), and Fath and Hassan (2011), studied the reheat cycle of the thermal vapor compression-multiple effect distillation (MED-TVC). Lee et al. (2002), presents a dynamic model for MED process with horizontal-falling-film evaporators to predict the transient behaviors. Based on the time-scale analysis , a dynamic model is proposed, and dynamic simulation is performed with detailed features taken into consideration.

Reddy et al. (1995) studied the horizontal tube falling-film evaporators (HTFFE). Dynamic behavior of the HTFFE plant was developed, and used in predicting the dynamic behavior of the plant in control application. Further, performance optimization study is carried out for a typical six effect plant, using the dynamic programming technique to evaluate an optimal control policy of boiling temperatures in the various effects, in order to maximize the production capacity.

Aly et al. (1997) developed a dynamic model for MED process to study the transient behavior of the system. This model allowed the study of system start-up, shutdown, load changes and troubleshooting in which the plant performance changed significantly. The effect of feed flow, feed temperature and live (heating) steam flow changes on plant performance such as temperature, brine salinity, product flow rate, and brine level.

In present study, the transient and dynamic simulations using the solar thermal energy, without heat storage system, to drive the low temperature MED-TVC is presented. The operation mode is studied to demonstrate time dependence of the feed water flow rate behavior onto MED effects.

MED-TVC SYSTEM DESCRIPTION

The studied MED-TVC plant (Figure 1) consists of seven effects with main condenser and two feed water pre-heaters. The recycled entrained vapor is extracted from the fourth effect to mix with the motive steam inside the TVC. A third pre-heater uses the vacuum steam jet ejector condenser to further heat the feed water. The rejected brine from each effect is flashed into the next effect to add a new quantity of generated vapor. There are two values of feed water for effects, that is, 201.7 kg/s for the first four effects and 83.6 kg/s for last three effects, where the accumulated total feed water is 1057.5 kg/s. The feed water pump is used to pump the seawater with 3085 kg/s into the main condenser to condense the generated vapor in the last effect. Part of the heated seawater is used as feed water for the seven effects; while the rest water is rejected to the sea again after mixing with the brine below down to reduce the rejected flow salinity. Tables 1 and 2 summarize the system steady state technical specifications. The TVC entrained vapor is 21.1 kg/s, while the motive steam is 45.4 kg/s. The total water production of MED system is 300 kg/s. The recovery ratio for this system is 28.4 % and the Gain Output Ratio (GOR) is 8.5.

The generated vapor by boiling/evaporation of the feed water or by flashing the brine, both are mixed together then condensed to produce the distillate water plant production. The quantity of mass flow of the entrained vapor, after condensed in the first effect, is returned to mix with water production. The condensed mass flow of

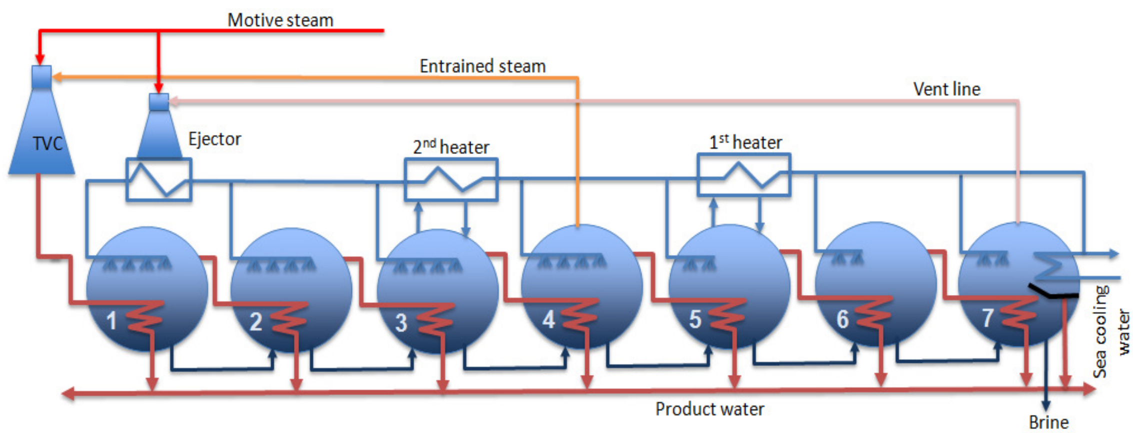

Figure 1. Schematic flow diagram of 25900 m^3/d MED-TVC plant.

Table 1. Overall technical specification of the MED-TVC plant.

Parameter	Value
Top brine temperature (°C)	65.6
Heating steam flow rate (kg/s)	66.4
Distillate water flow rate (kg/s)	300.0
Brine flow rate (kg/s)	733.2
Recovery ratio (%)	28.4
Gain output ratio (GOR)	8.5
Seawater temperature (°C)	35.0
Seawater flow rate (kg/s)	3085.0
Feed water flow rate (kg/s)	1057.5
Rejected water flow rate (kg/s)	2027.5
Rejected salinity (ppm)	53381.6
Seawater salinity (ppm)	48200.0

motive steam is returned back to heating system to gain new thermal power.

TRANSIENT AND DYNAMIC SYSTEM OPERATION

Typical solar intensity

The data used in the simulations are for Abu Dhabi collected from the weather station at Masdar City in the summer where the data is the average for the month of July 2010. In Figure 2, curve fitting was used for the data in MS Excel and the polynomial function as defined in Equation 1 was used in the simulation.

$$I(t) = 2.04407e^{-15} * \text{Time}^4 - 2.115872e^{-10} * \text{Time}^3 + 5.503613e^{-6} * \text{Time}^2 - 2.001969e^{-3} * \text{Time} - 3.519359) * 1.136 \quad (1)$$

System transient conditions

The solar driven MED-TVC system obtains its heat source from sun radiation along hours of the day. The sun thermal power sine wave is assumed with the steady-state value of 155.4 MW, as the maximum value at mid-day (Figure 3).

The electrical power is generated from a solar-PV system for pumping. Two scenarios for Solar-MED feeding the feed water into the effects are studied (Figure 4) as follows:

(a) In the first scenario, the feed water is pumped as constant value most of the operation period and independent on the time or the solar intensity, green line of Figure 4a. At the beginning of operation, all quantity of condenser cooling seawater is used as feed water until its value reach to steady-state value of condenser cooling (1057.6 kg/s). The excess cooling seawater is rejected to sea to keep the feed water at steady-state constant value. Near the end of the day, and once the cooling seawater reaches back the feed water value of 1057.6 kg/s, all seawater is used back as feed with no seawater rejected to the sea.
(b) In the second scenario, the feed water is pumped fully following the solar sinusoidal curve as shown in

Table 2. Steady-state technical specification for each effect.

Parameter	Number of effects						
	1	**2**	**3**	**4**	**5**	**6**	**7**
Brine temperature (°C)	65.6	62.4	59.2	56.1	52.0	47.8	43.7
Boiling point elevation (°C)	0.78	0.77	0.75	0.73	0.71	0.69	0.67
Feed water temperature (°C)	61.8	56.5	56.5	49.3	49.3	41.0	41.0
Feed water flow rate (kg/s)	201.7	201.7	201.7	201.7	83.6	83.6	83.6
Vapor flow rate (kg/s)	64.9	62.8	62.3	54	34.3	24.3	27.2
Brine salinity (ppm)	71091.5	70703.2	70602.0	69415.8	70648.2	70652.5	70947.7

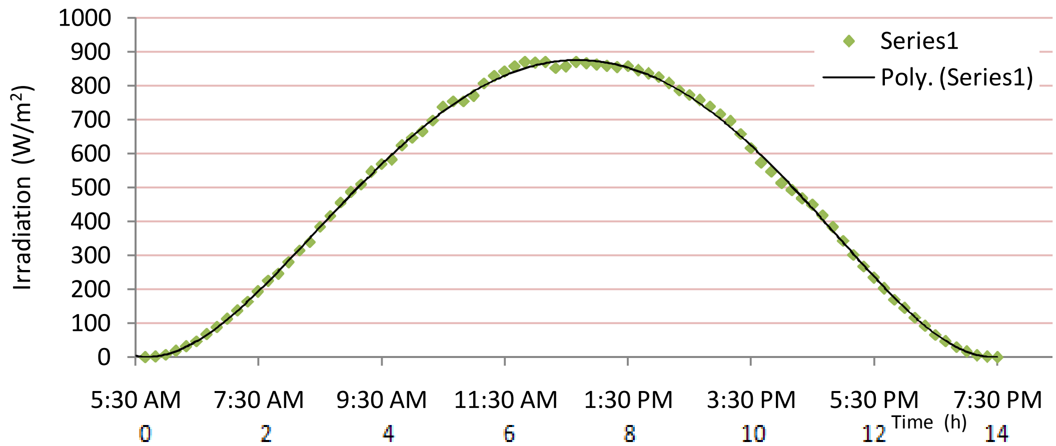

Figure 2. Irradiation at summer conditions - Abu Dhabi.

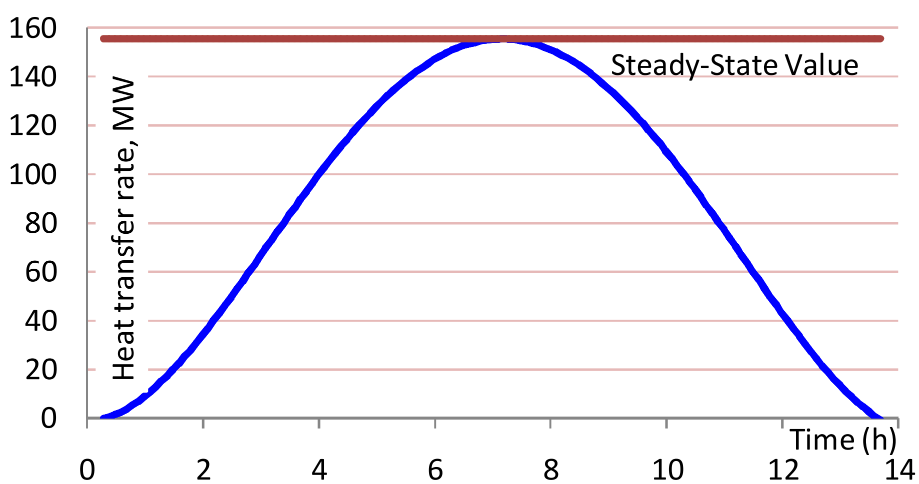

Figure 3. Heat transfer rate of the input heating steam into the 1st effect.

Figure 4b, with midday peak value equal to the steady-state value of 1057.6 kg/s. The three streams of the seawater, rejected water and the feed water are operated and shut down almost altogether during the operation period.

There are two periods in the daily operation; at start-up and shut-down, in these two periods there is no production of distillate due to the conditions of heating steam is insufficient enough to operate the system. The duration of the two periods is not the same for the t wo

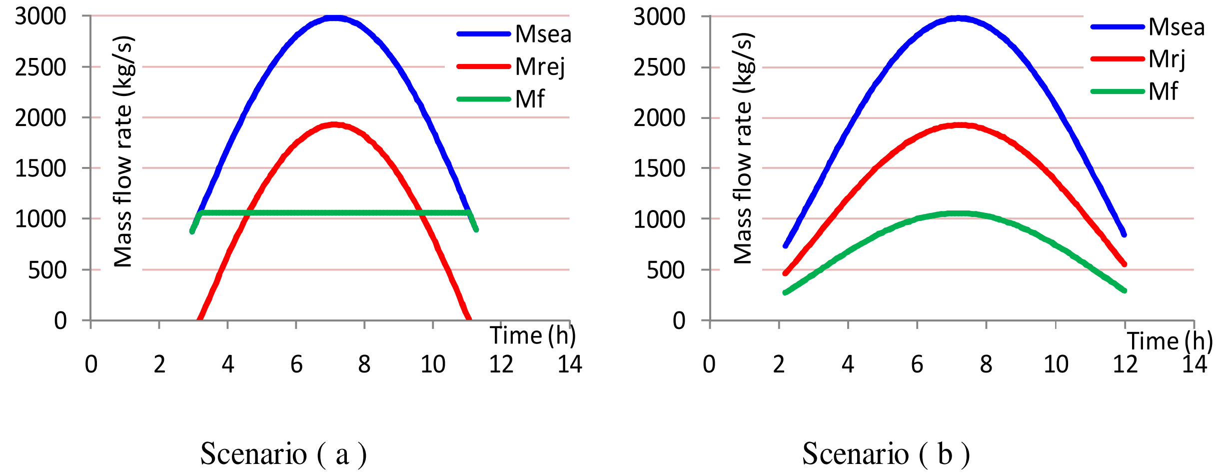

Figure 4. Transient simulation of the mass flow rates of seawater, rejected water to the sea and feed water for the effects.

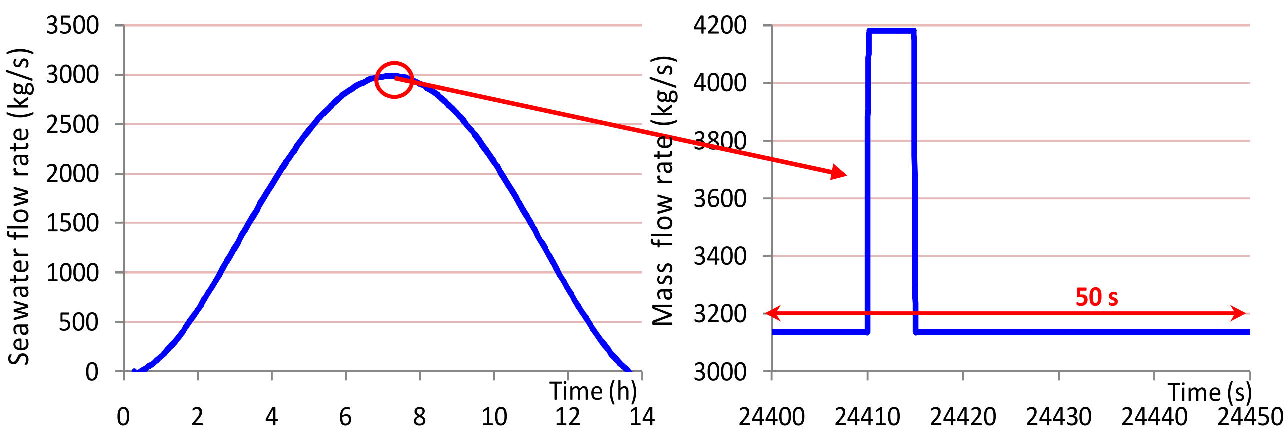

Figure 5. Employed disturbance of the pulse forcing function for seawater flow rate.

scenarios, as clear in Figure 4a and b.

Applied dynamic forcing function

Figure 5, represents the forcing function that applied on the pumped seawater into the condenser which the peak value of the seawater is 3085 kg/s. The applied forcing function simulates increasing the seawater flow rate from steady state value to 4122 kg/s for five second. The applied forcing function started at 24410th s and finished at 24415th s. In this study, the total testing period 50 s including the forcing time of disturbance and steady operation before and after forcing time, as shown in Figure 5. The dynamic simulation procedure for the MED-TVC system has been derived by writing the differential terms in the stage model equations and the forcing function in finite difference form.

MATHEMATICAL MODEL

The developed transient simulation mathematical model (to analyze solar driven MED-TVC) takes into consideration the variation of the physical properties of the brine due to change of the temperature and salt concentration.

As shown in Figure 6, the change in brine mass flow rate ($M_{B,i}$) in the brine pool of effect (i) is formed by the balance of time behavior of four streams; the sprayed feed water into the effect ($M_{F,i}$), brine flow from the previous effect ($M_{B,i-1}$), generated vapor by boiling in the effect ($M_{VB,i}$) and the generated vapor by flashing in the effect ($M_{VF,i}$), as the following equation:

$$\frac{\partial}{\partial t}M_{B(i)} = \frac{\partial}{\partial t}M_{F(i)} + \frac{\partial}{\partial t}M_{B(i-1)} - \frac{\partial}{\partial t}M_{VB(i)} - \frac{\partial}{\partial t}M_{VF(i)} \quad (2)$$

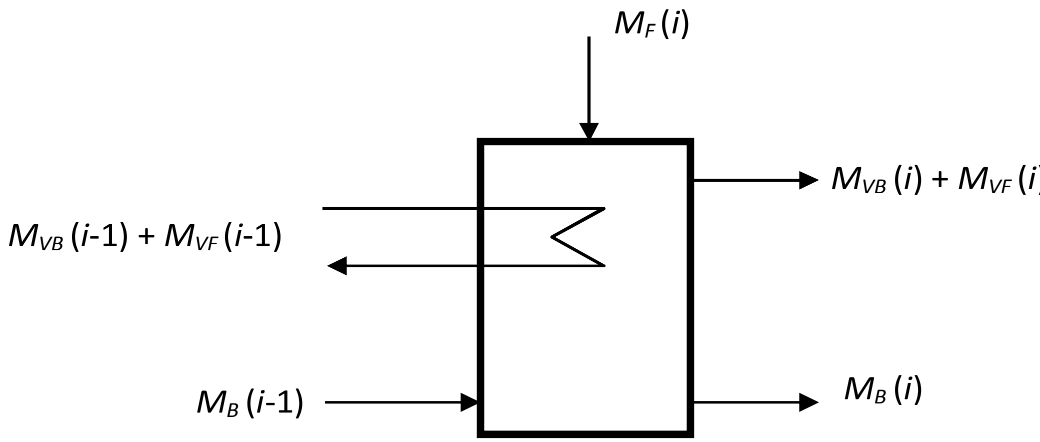

Figure 6. Physical model of the effect (i), mass balance.

$$\frac{\partial M_{VB(4)}}{\partial t} = \frac{\partial}{\partial t}\left(\frac{\left(M_{VB(3)} - M_{Ven(3)} - M_{Ch(3)} + M_{VF(3)}\right)E_{VBfg\,(3)} - M_{F(4)}C_{P(4)}\left(T_{B(4)} - T_{F(4)}\right)}{E_{VBfg\,(4)}}\right) \quad (3)$$

As shown in Figure 1, each effect has different input out streams. So, there is a different mathematical form to calculate the generated vapor in each effect. For example, Equation 3 represents the dynamic behavior of mathematical model for the generated vapor in effect (Equation 4) by boiling process from the feed water using the energy balance.

The differential equation (4), of the outlet (rejected) temperature of the condenser, for the seawater that used to condense all vapor generated in the last effect (*k*), can be expressed as:

$$\frac{\partial}{\partial t}T_{OCond} = \frac{\partial}{\partial t}\left(T_{Sea} + \frac{\left(M_{VB(k)} + M_{VF(k)} - M_{Ven(k)}\right)E_{VBfg(k)}}{M_{Sea}\,C_{Psea}}\right) \quad (4)$$

The rate of change of heating steam is:

$$\frac{\partial M_{Steam}}{\partial t} = \frac{\partial}{\partial t}\left(M_{OS} + M_{Vent}\right) \quad (5)$$

Then the time change of the top brine temperature in the first effect can be calculated as follows:

$$T_{TBT} = T_{f1} + \frac{M_{Steam}\,E_{St.fg} - M_{VB1}\,E_{VB1.fg}}{M_{f1}\,C_{Pf1}} \quad \mathbf{(6)}$$

RESULTS AND DISCUSSION

Transient simulation

The assumed mass flow rate of the heating steam will follow the sinusoidal curve with peak value of 66.4 kg/s (the steady state design value of the MED condition). Following to this transient esponse, the TVC motive steam and the entrained vapor mass flow rates will also follow the same sinusoidal trend for both feed water scenarios (a) and (b), as shown in Figure 7. The results of Figure 7 show that the difference between two feed water scenarios can be neglected except for the duration of the operating hours.

The generated vapor in the seven effects follows the same sinusoidal trend, as shown the Figure 8. The peaks values of the generated vapor present the value of the designed condition. There is no valuable difference between transient simulations for generated vapor in two scenarios. Two groups are shown in Figure 8, one for the first four effects (of large production) and the second three effects (of less production).

The resultant transient brine flow rates are shown in Figure 9. In scenario (a), where the feed water is sprayed into the effects at constant steady state value (most of the operating hours), the brine flow rate will follow the negative-trend of sine wave (constant feed and

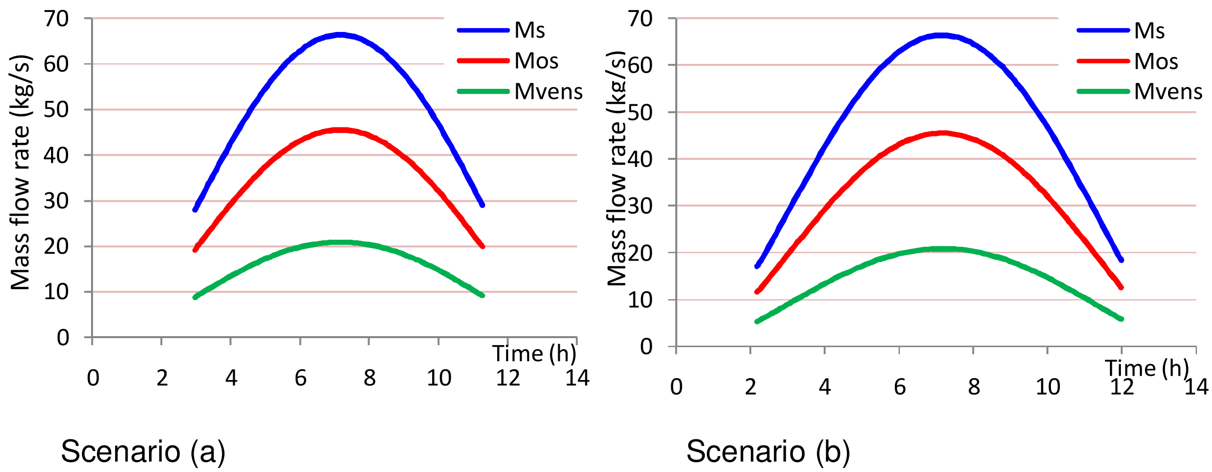

Figure 7. Transient mass flow rates of heating steam, motive steam and entrained vapor.

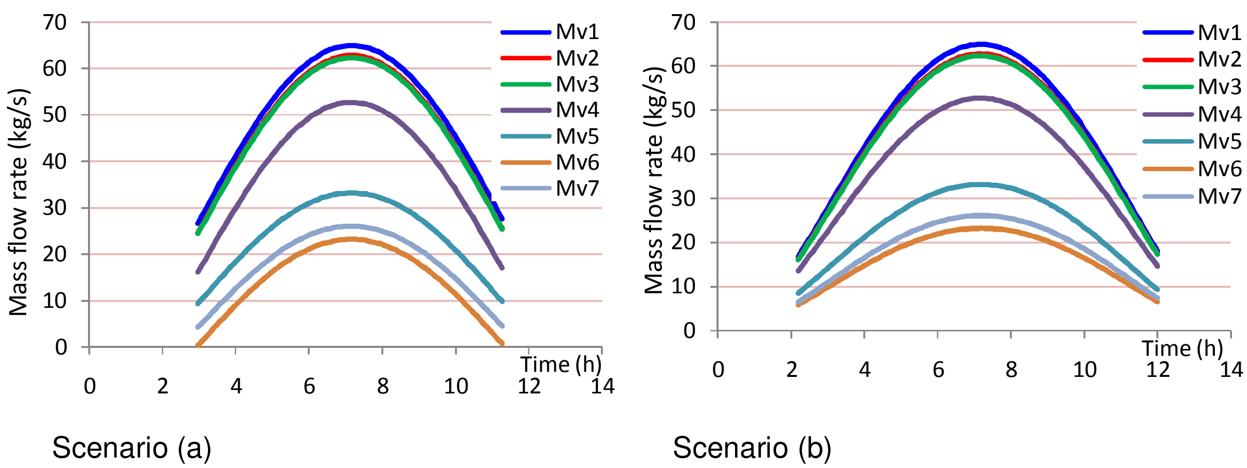

Figure 8. Transient Results of the generated vapor mass flow rate.

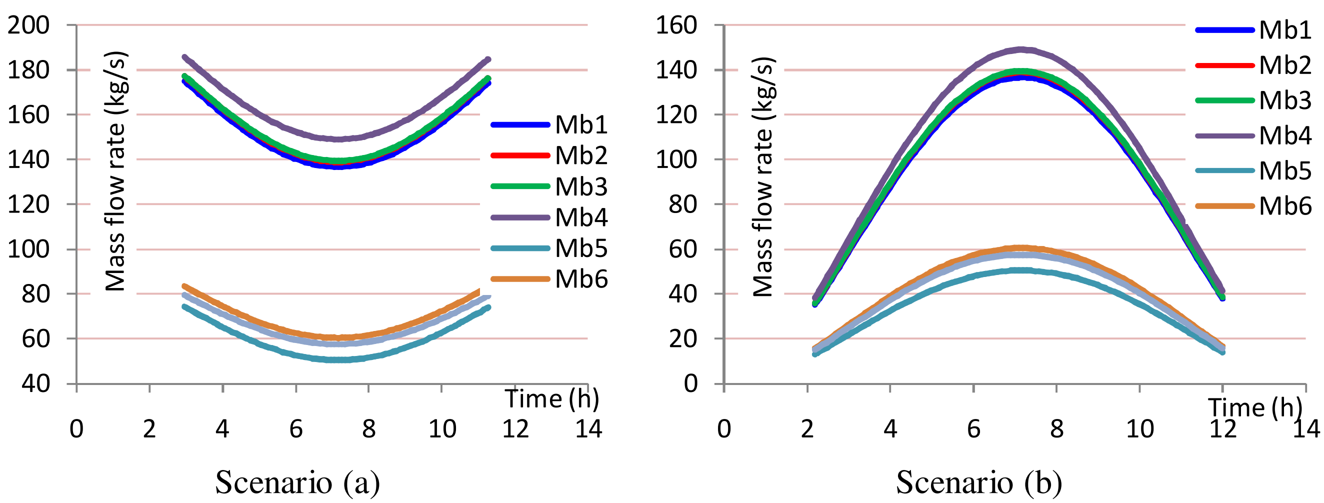

Figure 9. Transient results of the brine mass flow rate.

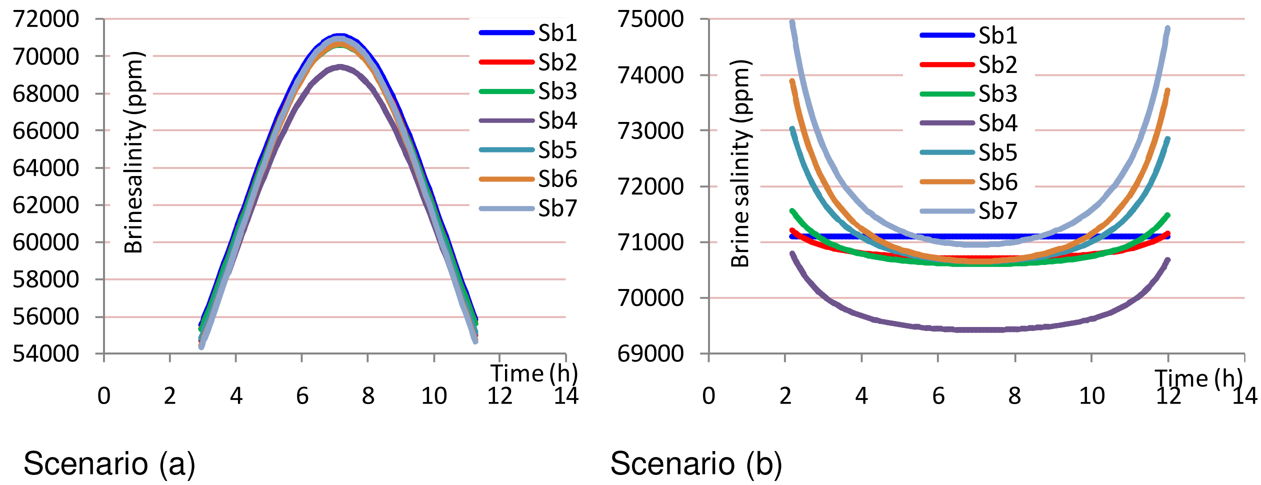

Figure 10. Transient simulation of brine salinity produced in each effect.

vapor production) with the midday lowest values represent the values of design condition (Figure 9a). Whilst in the second scenario (b), where the feed follows the sine wave, the transient brine flow rates will follow the shape of positive-sine wave (Figure 9b) with the peak values represent the values of design condition. Figures 10 represent the transient brine salinity for each effect. In general, the lowest value of brine flow rate (Figure 9) represents the highest value of brine salinity. The peak values of Figure 10a show the salt concentration with the maximum value at around 71000 ppm in the first effect, this value is equal to the MED design value. While in Figure 10b, the brine concentration in the last effect reached to 75000 ppm at the start and the end of the operating hours. On the other hand, the first effect is completely stable with any change in salt concentration of designed value. So, the last effects face a problem of salt precipitation rate higher than the first ones and there is a need to increase the feed water flow rate to control the high salinity near the start-up and shut-down periods.

Dynamic simulation

Nearly at around the midday, the time response of the rejected seawater flow (that goes out from the condenser) is affected by the disturbance which increasing gradually from normal operation value then decreasing again to the same value (Figure 11). This dynamic behavior for rejected seawater is very close to dynamic behavior having been happened for the seawater supply. The system undergoes this disturbance is still stable in operation because the change in its behavior is just bounded around the disturbance time, and regain in a very short time. Meanwhile, the dynamic behavior of the rejected seawater temperature is also decreased due to its mass flow increased, as shown in Figure 12.

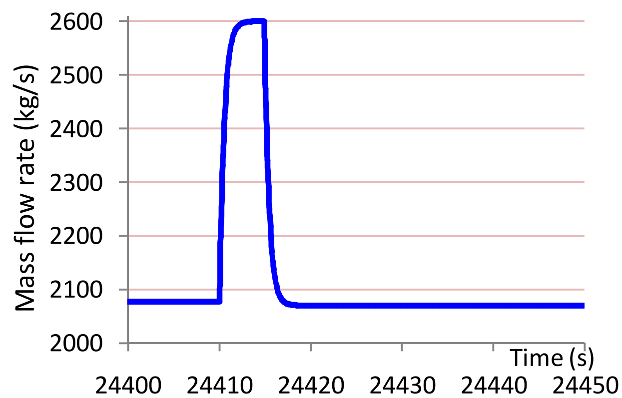

Figure 11. Time response of rejected seawater mass flow rate.

The dynamic behavior of the second part of outlet cooling seawater, which it selected as a feed water line to feed the effects is shows in Figure 13. The accumulated feed water of 1057.5 kg/s is increased before entering effect-7 with highest value. Once effect-7 is fed, the behavior of the rest feed water is disturbed with a value less than the previous part, and so on. The disturbance in the 1st effect has the lowest value of dynamic change. This dynamic behavior undergoes the behavior of inter-relationship between all components of the system due to the change of time span needed for each component to cause an interrelation feedback response from first and last effect.

The design values of the feed water flow rate to the first four effects are 201.7 kg/s while the last three effects are 83.6 kg/s. So, and as shown in Figure 14, the dynamic behavior of the mass flow rate of last effect is increased

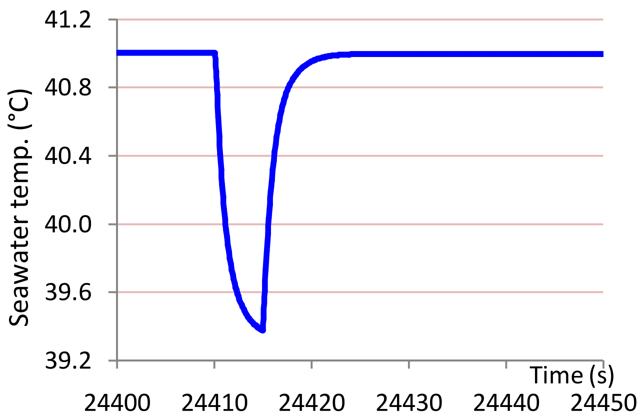

Figure 12. Dynamic behavior of rejected seawater temperature.

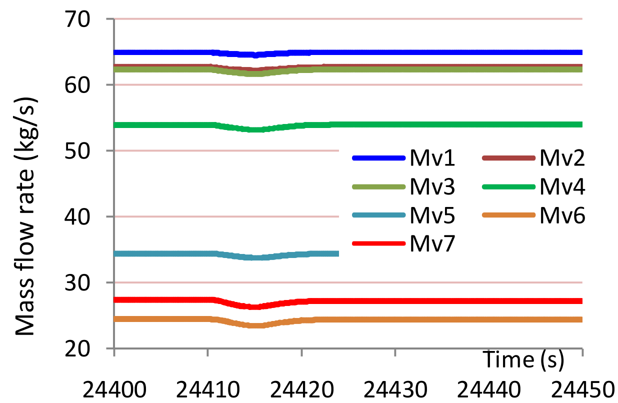

Figure 15. Dynamic simulation for generated vapor by boiling process in each effect.

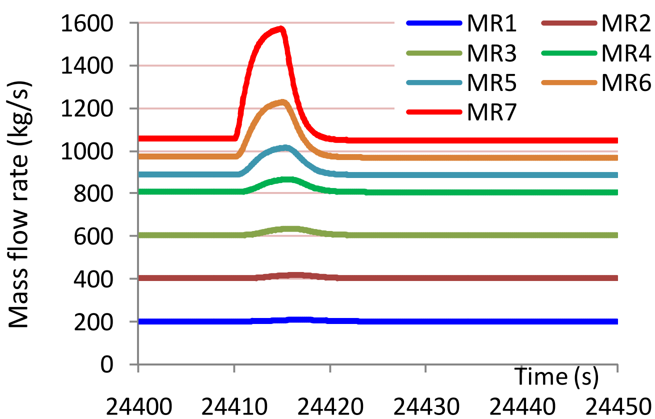

Figure 13. Time response of mass flow rate in feed water line.

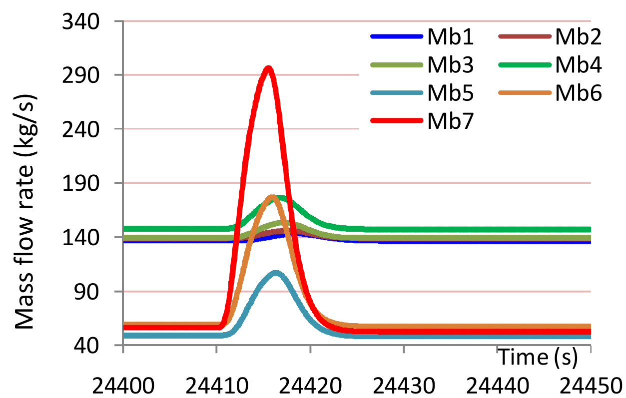

Figure 16. Dynamic simulation for mass flow rate of the rest brine per effect.

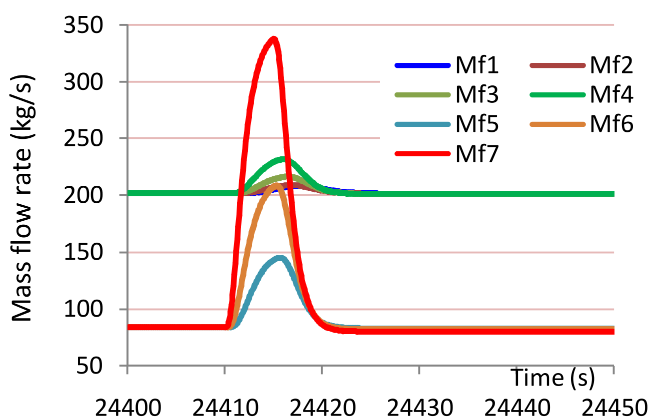

Figure 14. Dynamic simulation for sprayed feed water in each effect.

gradually smoother than the rejected seawater. Also, the dynamic behavior undergoes the last effect is greater than the previous one (6th effect), while the change in 6th effect is greater than the 5th effect, and so on. The dynamic simulation of the feed water follows the dynamic simulation of the rejected seawater because they are two parts of the same seawater flow.

As a result of the increasing the dynamic behavior of the feed water flow and also decreasing its temperature, the behavior of the generated vapor mass flow rate by boiling, will be decreased as shown in Figure 15. Following to this response and as shown in Figure 16, the behavior of rest brine mass flow rate follows the response of the feed water and generated vapor which the brine flow will increase due to decrease the vapor as increase in feed water.

Figure 17, shows the rate of change of heating steam (*DMs*), entrained vapor from the fourth effect (*DMvens*), and the motive steam (*DMos*). Due to decrease of response of generated vapor flow rate, the response of the entrained flow rate from fourth effect to mix with motive steam inside TVC will also decrease. Then, the response of heating steam as a product of mixing of

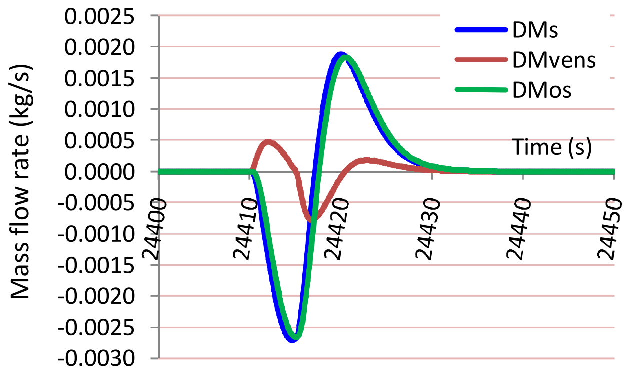

Figure 17. Change rate in mass flow rate of heating steam, motive steam and entrained vapor.

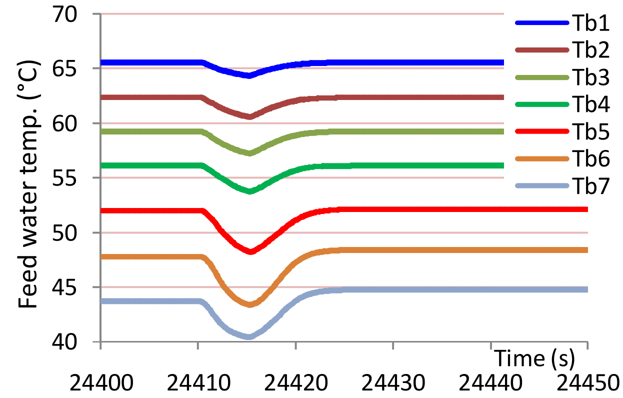

Figure 20. Dynamic behavior of brine temperature.

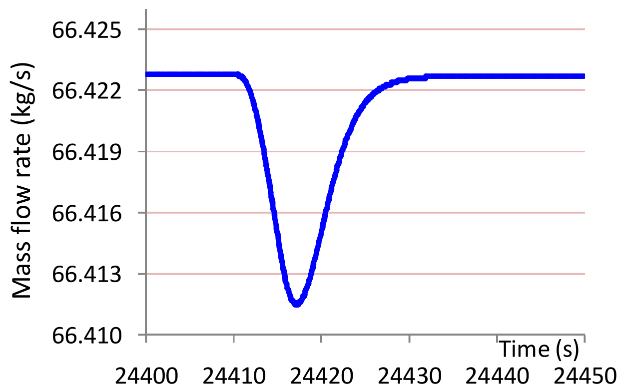

Figure 18. Time change in mass flow rate of heating steam into 1st effect.

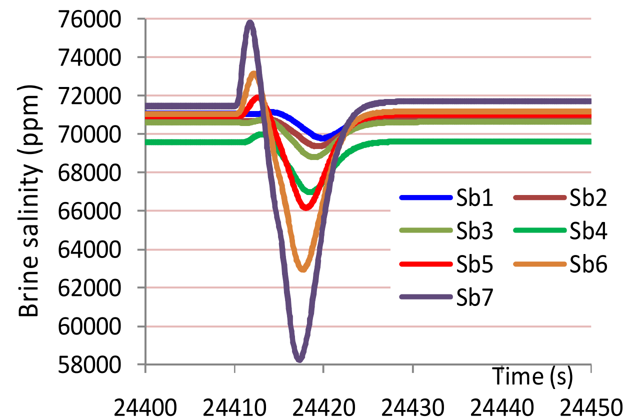

Figure 21. Simulation of brine salinity.

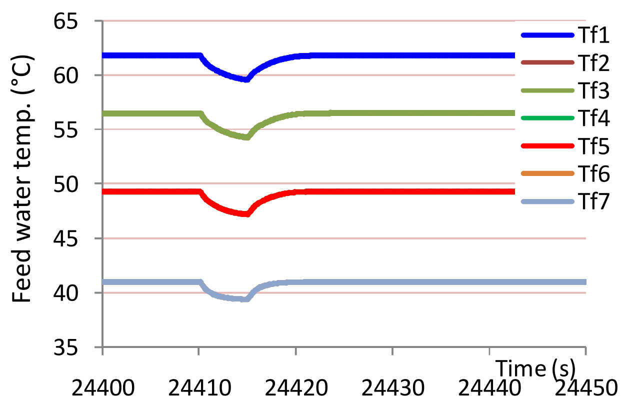

Figure 19. Time response of feed water temperature.

motive steam and entrained vapor will also decrease as shown in Figure 18. This will further decrease and vapor production in each effect or there will be a need for addition rate of heating steam.

Similarly, the dynamic simulation of the feed water temperature followed the dynamic simulation of the rejected seawater temperature because they are two parts of the one flow. In this MED-TVC system and as mentioned in Table 2, there are four different values of responses of dynamic behavior for the feed water temperature as a result of operating of three feed water preheaters, as shown in Figure 19. In addition, the response of brine temperature is decreased as a result of increasing the brine flow rate, decreasing the heat source in each effect and decreases the temperature of feed per each effect, as shown in Figure 20.

Finally and according to the studied configuration of MED-TVC design and the type of applied disturbance, there is a high probability to salt precipitation on last effects. This probability is decreased from last effect to the first one, as shown in Figure 21. Also, the dynamic behavior of the *GOR* will be decreased, as shown in Figure 22. In a way, it similar to heating steam trend in Figure 18.

Conclusions

The transient and dynamic simulations for a typical operating MED-TVC system have been carried out.

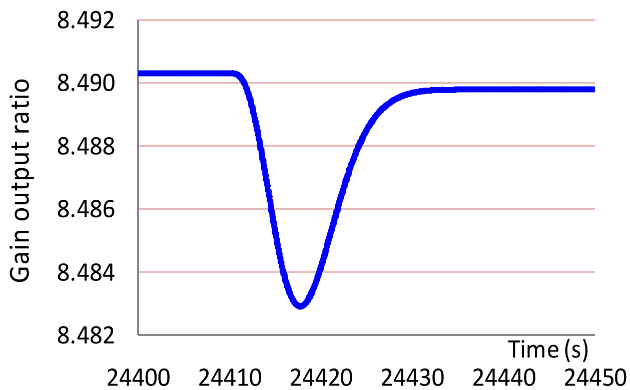

Figure 22. Time change in gain output ratio.

Without any disturbance, the dynamic model predicts a steady state. The diagnostic analyses of the numerical simulation can summarized as:

1. The sinusoidal transient solar thermal power as an input energy to drive MED desalination plant shows a higher salt precipitation rate than the design value on the last effects. Sinusoidal feed water flow rate is the better solution for the safe operation (of acceptable brine concentration and salts precipitation).
2. The system is affected by the applied disturbance and increases gradually from normal operation then decreases back to the normal operation value. The system undergoes this disturbance is still stable in operation as the change in its behavior is just bounded around the disturbance time, and regain in a very short time is working at steady-state value of starting point.
3. The last effects face a problem of slat precipitation higher than the first ones in case of the sinusoidal feeding for seawater stream.
4. A dynamic behavior methodology is a good tool to predict features of the systems and can also prove if the system is stable or not. This study shows that the MED-TVC plant is a stable system.

Abbreviations: $\mathbf{C_p}$, Specific heat at constant pressure (kJ/kg. ℃); $\mathbf{C_{P,I}}$, specific heat at constant pressure in effect (i) (kJ/kg.℃); $\mathbf{C_{Pf1}}$, specific heat at constant pressure for feed water into the first effect (kJ/kg.℃); $\mathbf{C_{Psea}}$, specific heat at constant pressure for seawater (kJ/kg.℃); $\mathbf{DM_{OS}}$, rate of change of mass flow rate of motive steam (kg/s); **DMs,** rate of change of mass flow rate of heating steam (kg/s); **DMven,s,** rate of change of mass flow rate of entrained vapor from fourth effect (kg/s); $\mathbf{E_{St,fg}}$, latent heat enthalpy of the heating steam (kJ/kg); $\mathbf{E_{VB1,fg}}$, latent heat enthalpy of the vapor in the first effect (kJ/kg); $\mathbf{E_{VBfg,I}}$, enthalpy of the vapor released from the brine in effect (i) (kJ/kg); **GOR,** gain output ratio; $\mathbf{h_{fg}}$, latent heat (kJ/kg); **I,** selected effect; **k,** last effect or total number of effects; $\mathbf{M_b}$, brine mass flow rate (kg/s); $\mathbf{M_{B,I}}$, mass flow rate of brine in the brine pool of effect (i) (kg/s); $\mathbf{M_{Ch,I}}$, mass flow rate of condensed vapor for heating the feed water inside the preheater (i) (kg/s); **Md,** mass flow rate of distillate water (kg/s); $\mathbf{M_f}$, total mass flow rate of feed water for all effects (kg/s); $\mathbf{M_{F,I}}$, the sprayed mass flow rate of feed water onto the horizontal tubes in effect (i) (kg/s); $\mathbf{M_{OS}}$, mass flow rate of motive steam (kg/s); **Mrj,** mass flow rate of rejected water to the sea (kg/s); **Ms,** mass flow rate of heating steam (kg/s); $\mathbf{M_{Sea}}$, mass flow rate of the seawater into the condenser (kg/s); **Msea,** mass flow rate of seawater (kg/s); $\mathbf{M_{Steam}}$, mass flow rate of heating steam (kg/s); **Mv,** generated vapor mass flow rate (kg/s); $\mathbf{M_{VB,I}}$, the vapor released from the feed water in effect (i) (kg/s); $\mathbf{M_{Ven,I}}$, mass flow rate of entrained vapor from i^{th} effect (kg/s); **Mvens,** mass flow rate of entrained vapor from fourth effect (kg/s); $\mathbf{M_{Vent}}$, mass flow rate of entrained vapor from the fourth effect (kg/s) $\mathbf{M_{VF,I}}$, The generated vapor released by flashing process in effect (i) from the brine that comes from the previous effect (i-1) (kg/s); **Qs,** heat transfer rate in the first effect (W); **RR,** recovery ratio; $\mathbf{S_b}$, brine salinity (ppm); $\mathbf{T_b}$, brine temperature (℃); $\mathbf{T_{B,I}}$, brine temperature in effect (i) (℃); $\mathbf{T_f}$, feed water temperature (℃) $\mathbf{T_{F,I}}$, Feed water temperature in effect (i) (℃); $\mathbf{T_{OCond}}$, temperature of the outlet (rejected) flow of the condenser for the seawater (℃).

REFERENCES

Al-Hallaj S, Parekh S, Farid MM, Selman JR (2006). “Solar desalination with humidification-dehumidification cycle: Review of economics,” Desalination, 195(1): 169–186.

Ali El-Nashar M (2008). "Multiple effect distillation of sweater using solar energy", Book, Nova science publishers, Inc., New York,

Aly NH (1997). “Dynamic Response of Multi-Effect Evaporators”, Desalination, Vol. 114.

Hassan AS, Hanafi AS (2007). "Dynamic Behavior of Multiple Effect Distillation with the Disturbance of Seawater Mass Flow Rate", IDA World Congress, Maspalomas, Gran Canaria, Spain, pp. 21-26.

Fath HES, Hassan AS (2011). "Transient Simulation of Solar Driven Multiple Effect Distillation Plant (Solar-MED)", IDA World Congress – Perth Convention and Exhibition Centre (PCEC), Perth, Western Australia.

Hassan F, El-Sherbiny S, Hassan A, Rommel M, Wieghaus M, Koschikowski J, Vatansever M(2008). “PV and Thermally Driven Small-Scale, Stand-Alone Solar Desalination System with very Low maintenance Needs”, Desalination, 225: 1-3, 58-69.

Kalogirou SA (2004). “Solar thermal collectors and applications”. Progr. Energy Combustion Sci., 30(3): 231–295.

Mabrouk AA, Nafey AS, Fath HES (2008). “Thermo economical Design of a Multi Effect Evaporation – Mechanical Vapor Compression (MEE-MVC) Desalination Process”. Desalination, 230: 1-3, 1-15.

Tauha AM, Hassan FES, Peter AR (2011). "A Comprehensive Techno-economical Review of Indirect Solar Desalination". Renewabl Sustain. Energy Rev., 15: 4187-4199.

Reddy KV (1995). “Dynamic Modeling of the MSF Desalination Process”, IDA world congress on desalination and water sciences, Abu Dhabi.